*metals*

MDPI

*Article*

# Kinetics of Aluminum and Scandium Extraction from Desilicated Coal Fly Ash by High-Pressure HCl Leaching

**Andrei Shoppert [1,*], Dmitry Valeev [2] and Irina Loginova [3]**

[1] Laboratory of Advanced Technologies in Non-Ferrous and Ferrous Metals Raw Materials Processing, Ural Federal University, 620002 Yekaterinburg, Russia
[2] Laboratory of Sorption Methods, Vernadsky Institute of Geochemistry and Analytical Chemistry of the Russian Academy of Sciences, 119991 Moscow, Russia; dmvaleev@yandex.ru
[3] Department of Non-Ferrous Metals Metallurgy, Ural Federal University, 620002 Yekaterinburg, Russia; i.v.loginova@urfu.ru
* Correspondence: a.a.shoppert@urfu.ru

**Abstract:** Coal fly ash (CFA) is a waste that forms via coal combustion in thermal power stations. CFA consists of numerous components, whose recovery can address environmental and resource concerns associated with sustainable development. Most of the alumina ($Al_2O_3$) and rare-earth elements (REEs) in CFA are contained in the amorphous glassy mass and in the refractory mullite phase ($3Al_2O_3 \cdot SiO_2$), which can be dissolved only using high-pressure acid leaching (HPAL). In this paper, the method of preactivation of CFA by treatment with a highly concentrated NaOH solution is used to increase the efficiency of Al and Sc extraction during HPAL. This method allows for the elimination of an inert aluminosilicate layer from the surface of mullite, transferring the REEs into an acid-soluble form. The Al and Sc extraction can reach 80% after HCl HPAL at T = 170 °C and a 90 min duration. According to the kinetic data, the dissolution of Al follows the surface chemical reaction and intraparticle diffusion shrinking core models in the initial and later stages of leaching, respectively. A high activation energy of 52.78 kJ $mol^{-1}$ was observed at low temperatures, and a change in the mechanism occurred after 170 °C when the activation energy decreased to 26.34 kJ $mol^{-1}$. The obtained activation energy value of 33.51 kJ $mol^{-1}$ for Sc leaching indicates that diffusion has a strong influence at all studied temperatures. The residue was analysed by SEM-EDX, XRF, BET, and XRD methods in order to understand the mechanism of DCFA HPAL process.

**Keywords:** coal fly ash; hydrochloric acid; desilication; kinetics; shrinking core model; Al extraction; Sc extraction



**Citation:** Shoppert, A.; Valeev, D.; Loginova, I. Kinetics of Aluminum and Scandium Extraction from Desilicated Coal Fly Ash by High-Pressure HCl Leaching. *Metals* **2023**, *13*, 1994. https://doi.org/10.3390/met13121994

Academic Editor: Daniel Assumpcao Bertuol

Received: 19 November 2023
Revised: 4 December 2023
Accepted: 7 December 2023
Published: 9 December 2023



## 1. Introduction

Coal ash (CA) is a waste generated via the process of coal combustion in thermal power plants (TPP). More than a billion tons of CA are produced each year in the world [1,2]. The chemical composition of CA varies based on the coal deposit and the method of coal combustion [3,4]. Regardless of the combustion method, CA contains a large amount of aluminum oxide and REEs, which makes it a promising raw material for smelter-grade alumina and REE concentrate production. The CA also contains up to 65 wt.% of silica, which prevents effective extraction of Al by alkaline methods. In addition, the CA obtained in pulverized coal boilers at T > 1100 °C transforms the aluminosilicates in coal into mullite, which can be dissolved in acid using hydrometallurgical methods only in a high-pressure reactor [5]. CA is also divided into bottom ash and fly ash—a fine fraction of ash, which is carried away with waste gases [6,7]. CFA yields more than 80%, and its fine composition eliminates the need for additional milling, so many studies have focused on extracting alumina from the fly ash [8,9].

In previous investigations, various approaches for CFA treatment for alumina extraction have been proposed, including alkaline [10–12], acidic [13–15], and combined, as

well as preliminary thermal activation [5,16] or sintering with an additive [17–19]. Acid methods are considered the most effective for high-silica raw materials treatment [20,21] as they allow for the silica to remain in the residue after the acid leaching, without the loss of Al and NaOH with the desilication product [22,23]. But, to recycle CFA from pulverized boilers, it is necessary to use an HPAL process at T > 200 °C [24]. It requires the use of more expensive equipment and increases energy consumption. It has been suggested to use mechanical activation [25,26], thermal treatment [27], or conversion of mullite to sodium aluminate by fusion with sodium compounds [28] to lower the leaching temperature, as this phase is easily dissolved into inorganic acids.

Our previous investigations have revealed that a novel method of CFA desilication employing a highly concentrated NaOH solution can eliminate the amorphous aluminosilicate layer from CFA particles without a highly alkali desilication formation [29,30]. The desilication process leads to an increase in the rare earth elements extraction from CFA by acid leaching, even at atmospheric pressure [31]. However, the Al extraction did not exceed 40%. This article is devoted to the investigation of Al extraction from desilicated CFA by the HPAL process at T = 150–190 °C using HCl, since it was shown [24] that HCl can immediately produce coagulants with a high added value compared to other acids. The effect of technological parameters, such as time and the ratio of liquid to solid (L:S ratio) on the extraction of Al and Sc, was studied. The experimental data that was obtained was processed using neural networks and a shrinking core model to examine the leaching kinetics and establish the mechanism of the HPAL process. The solid residue from CFA leaching was studied using scanning electron microscopy with energy dispersive analysis (SEM-EDS), X-ray phase analysis (XRF), laser diffraction (LD), and BET. The temperature of the HPAL process can be reduced from 210 °C to 170 °C with the same level of Al extraction by using preliminary desilication. Furthermore, it is shown that more than 90% of Sc can be extracted simultaneously.

## 2. Materials and Methods

### *2.1. Raw Materials*

CFA used in this investigation was taken from the Reftinskaya TPP in Asbest, Russia, where coal is pulverized into boilers for combustion at a temperature higher than 1300 °C. Table 1 shows the concentration of main components in CFA and CFA after desilication (DCFA) with NaOH at 110 °C, 20 min, an L:S ratio of 10:1, and an NaOH concentration of 400 g $L^{-1}$. Desilication was carried out with simultaneous magnetic fraction recovery [30]. Table 1 shows that the raw CFA is composed of 62.43 wt.% of $SiO_2$, 24.66 wt.% of $Al_2O_3$, and 3.32 wt.% of $Fe_2O_3$. After desilication with magnetic fraction recovery, the $Al_2O_3$ content increases to 44.30 wt.%, while the $SiO_2$ and $Fe_2O_3$ content reduce to 36.17% and 1.83%, respectively. The $Na_2O$ content in DCFA did not exceed 1 wt.%. Prior to conducting a kinetics investigation, DCFA underwent a sieving process to obtain a narrow particle size range of 50 µm to 73 µm. The $Al_2O_3$ and Sc content of this fraction was almost identical to DCFA and was 44.45% and 0.0041%, respectively. Figure 1 shows the results of XRD analysis of CFA and DCFA samples. Particle size distribution of DCFA can be found elsewhere [29,30].

**Table 1.** Concentration of main components in the Reftinskaya Thermal Power Plant (TPP) coal fly ash (CFA) and desilicated CFA (DCFA).

| Sample | Components (wt.%) | | | | | | | | | | |
|---|---|---|---|---|---|---|---|---|---|---|---|
| | $SiO_2$ | $Al_2O_3$ | CaO | $Fe_2O_3$ | $TiO_2$ | MgO | $Na_2O$ | $K_2O$ | LOI | Sc | C |
| Raw CFA | 62.43 | 24.66 | 1.60 | 3.32 | 1.12 | 0.43 | 0.72 | 0.94 | 3.70 | 0.0023 | 1.60 |
| Desilicated CFA | 36.17 | 44.30 | 3.40 | 1.83 | 1.85 | 0.86 | 0.92 | 0.08 | 7.30 | 0.0040 | 2.67 |

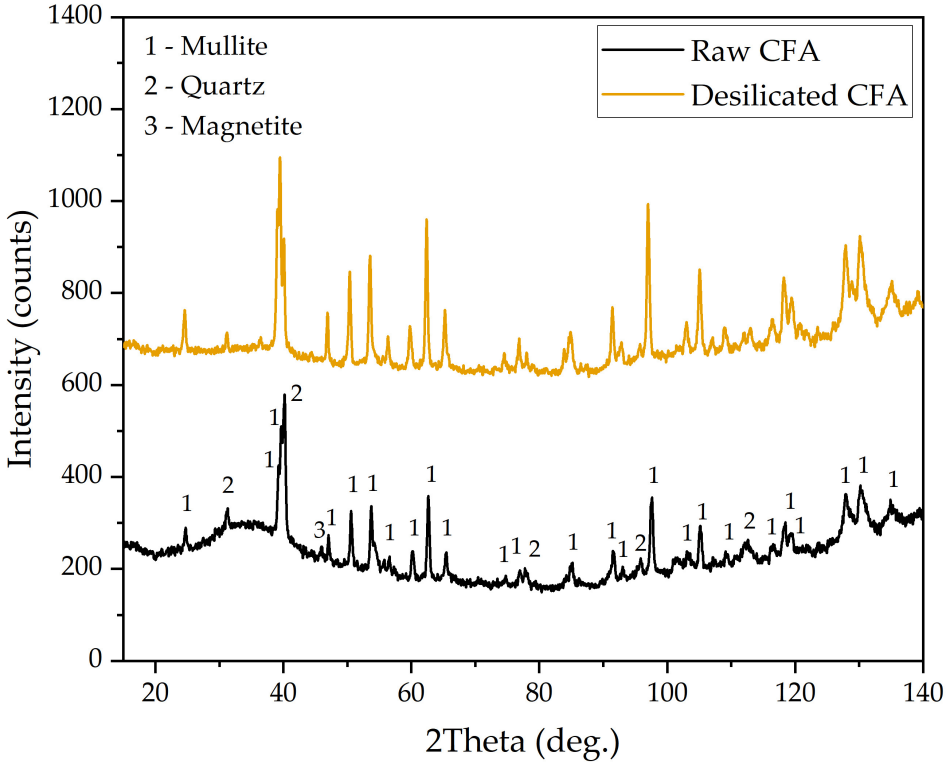


**Figure 1.** XRD patterns of the Reftinskaya TPP coal fly ash (CFA) and coal fly ash after desilication (DCFA).

The desilication process appeared to result in the absence of an amorphous glassy mass in DCFA (galo at 20–50° in the raw CFA). The morphology of DCFA particles was examined using SEM-EDX analysis (Figure 2). Figure 2 shows that DCFA consisted of spherical agglomerates of needle-shaped mullite particles. In this study, chemical reagents of analytical quality (NaOH and HCl) were used.

### *2.2. Experimental Procedure*

HPAL experiments were conducted using a DT-50 stainless-steel high-pressure reactor. A 50 mL beaker of fluoroplastic F4 was inserted into the reactor. The reactor was positioned in a 500 mL oil bath, which was mounted on a ZNCL-GS130 magnetic stirrer (Lichen Instrument Technology Co., Ltd., Shaoxing, China). An opening was made in the lid of the fluoroplastic beaker for the installation of a thermocouple. The thermocouple was placed 2 cm above the bottom of the beaker so it could accurately measure the temperature of the slurry during leaching. The slurry was stirred at 300 rpm using a magnet stirrer. The temperature of the oil was 220 °C at the time of heating. When the temperature in the reaction zone reached 150–190 °C, the temperature was fixed. The leaching reagent used was 30% hydrochloric acid. The L:S ratio was from 4:1 to 6:1. The leaching time at T = 150–190 °C was 30–90 min. In order to conduct kinetic studies, experiments were carried out with the selection of 7 points in the time interval of 15–90 min of leaching at a temperature range of 150–190 °C, with a step of 10 °C at a fixed L:S ratio of 5. Additionally, experiments were conducted at various L:S ratios ranging from 4 to 6, with a step of 1 at a fixed temperature of 170 °C. After leaching, the reactor was cooled for 15 min in cold running water until the slurry temperature decreased to 70 °C. Then, the reactor was opened, and the slurry was filtered. After washing, the residue was dried at T = 105 °C for 12 h.

A Box–Benken design was made using the software Statistica 13 (TIBCO, Hamburg, Germany) to minimize the impact of different variables on each other and diminish the number of tests. This design consisted of three blocks of 15 experiments. The variables

were adjusted at three distinct levels. The output parameters included the extraction of Al and Sc. A statistically driven, automated neural network (SANN) was employed to examine the impact of HCl leaching parameters on Al and Sc extraction from DCFA. The SANN modeling was executed using Statistica 13 software.

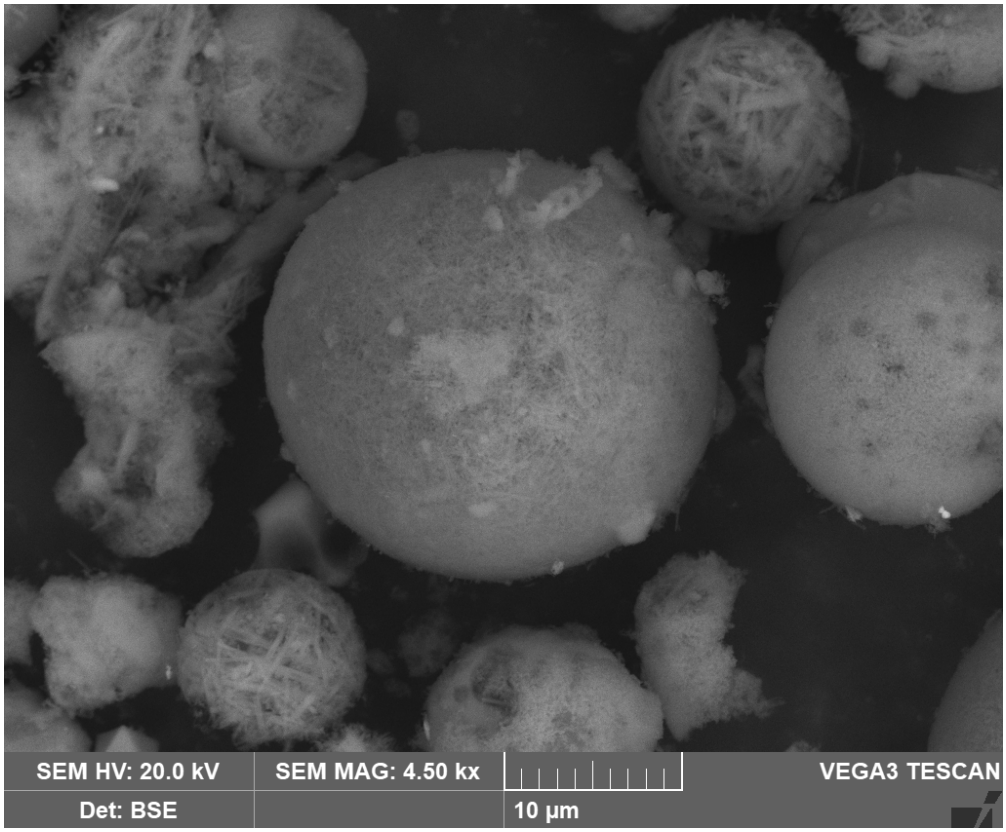


(**a**)

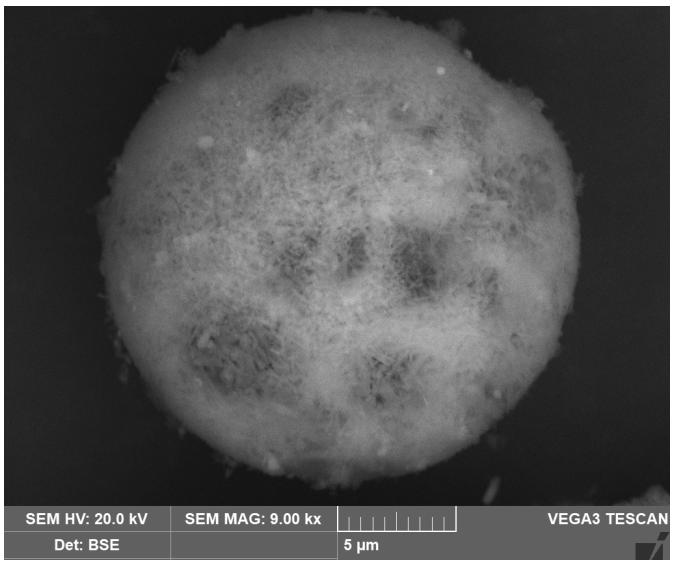


(**b**)

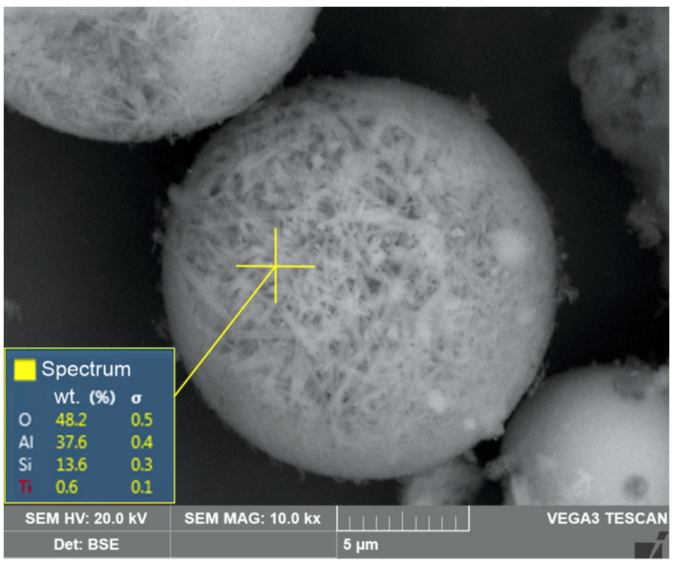


(**c**)

**Figure 2.** SEM-EDS images of (**a**) DCFA at a magnitude of 4500×; (**b**) mullite sphere at a magnitude of 9000×; (**c**) mullite sphere at a magnitude of 10,000×.

### 2.3. Analysis

The concentration of main components in DCFA and the residues obtained after HPAL were analysed by dissolution of the solid with a mix of concentrated hydrofluoric, sulphuric, and nitric acids. Then, the residue was fused with boric acid and soda. The fusing product was leached with 1 N HCl to obtain a solution for an inductively coupled plasma optical emission spectrometry (ICP-OES) analysis on a Vista Pro spectrometer (Varian Optical Spectr., Mulgrave, Australia). The metal concentration in the acid solutions after leaching and slurry filtration was also measured using ICP-OES.

A Difrei-401 diffractometer (JSC Scientific Instruments, Saint Petersburg, Russia) was used to determine the main phase of DCFA and HPAL residue. The SEM images of the solid products were studied using SEM-EDX analysis on a Vega III (Tescan, Brno, Czech Republic). The determination of the specific surface area of the products was carried out by the BET method, employing NOVA 1200e (Quantachrome Instruments, Boynton Beach, FL, USA). Prior to BET analysis, all samples were degassed under vacuum for 6–8 h at 200 °C.

The amounts of Al and Sc extracted from DCFA (X) were calculated using Equation (1), as follows:

$$X = (m_1 \times X_1 - m_2 \times X_2)/(m_1 \times X_1), \quad (1)$$

where $m_1$ is the original sample amount (g); $X_1$ is the concentration of component in the original sample (%); $m_2$ is the leaching residue amount (g); and $X_2$ is the concentration of component in the residue (%).

## 3. Results and Discussion

### 3.1. The Effect of Variables on the Al and Sc Extraction from DCFA

Table 2 presents a matrix of experiments displaying the levels of the primary parameters and the extraction of Al and Sc obtained at these parameters. The experimental data were processed by a neural network. The most suitable network was a multilayer perceptron "3-10-2" (R2 = 98.6%), where "3" is the number of parameters, "10" is the number of hidden neutrons layers and "2" is the number of dependent parameters. The response surfaces for Al extraction are depicted in Figure 3.

**Table 2.** Experimental plan matrix.

| Time (min) | Temperature (°C) | L:S Ratio | Al Extraction (%) | Sc Extraction (%) |
|---|---|---|---|---|
| 90 | 170 | 4 | 75.7 | 82.6 |
| 60 | 150 | 4 | 64.7 | 69.7 |
| 90 | 150 | 5 | 71.0 | 70.5 |
| 60 | 170 | 5 | 76.2 | 76.3 |
| 60 | 190 | 6 | 85.7 | 88.4 |
| 60 | 190 | 4 | 82.8 | 86.2 |
| 60 | 170 | 5 | 76.7 | 76.9 |
| 90 | 170 | 6 | 80.9 | 86.7 |
| 30 | 170 | 4 | 54.7 | 69.3 |
| 30 | 190 | 5 | 84.3 | 84.5 |
| 60 | 170 | 5 | 76.5 | 77.7 |
| 30 | 150 | 5 | 62.1 | 78.6 |
| 60 | 150 | 6 | 60.4 | 73.9 |
| 30 | 170 | 6 | 59.5 | 75.5 |
| 90 | 190 | 5 | 88.6 | 87.0 |

Figure 3 illustrates that the leaching time and temperature exert a significant influence on the extraction of Al. The increase in leaching time from 30 to 90 min at 170 °C results in an increase in Al extraction from 55% to 79%. The increase in temperature from 150 to 190 °C results in an increase in the extraction of Al from 64% to 87% after 90 min of leaching. The increase in the L:S ratio from 4 to 6 at 170 °C results in an increase in Al extraction of only 11% after 90 min, as depicted in Figure 3b.

Figure 4 shows the response surfaces obtained by the model for extracting Sc from DCFA. The process temperature affects Sc extraction the most. Increasing the temperature from 150 to 190 °C increases the Sc extraction from 70% to 89% after 90 min of leaching. Increasing the time from 30 to 90 min at 170 °C increases the Sc extraction from 71% to 81%. Increasing the L:S ratio from 4 to 6 at the same temperature increases the Sc extraction from 79% to 82% after 90 min of leaching.

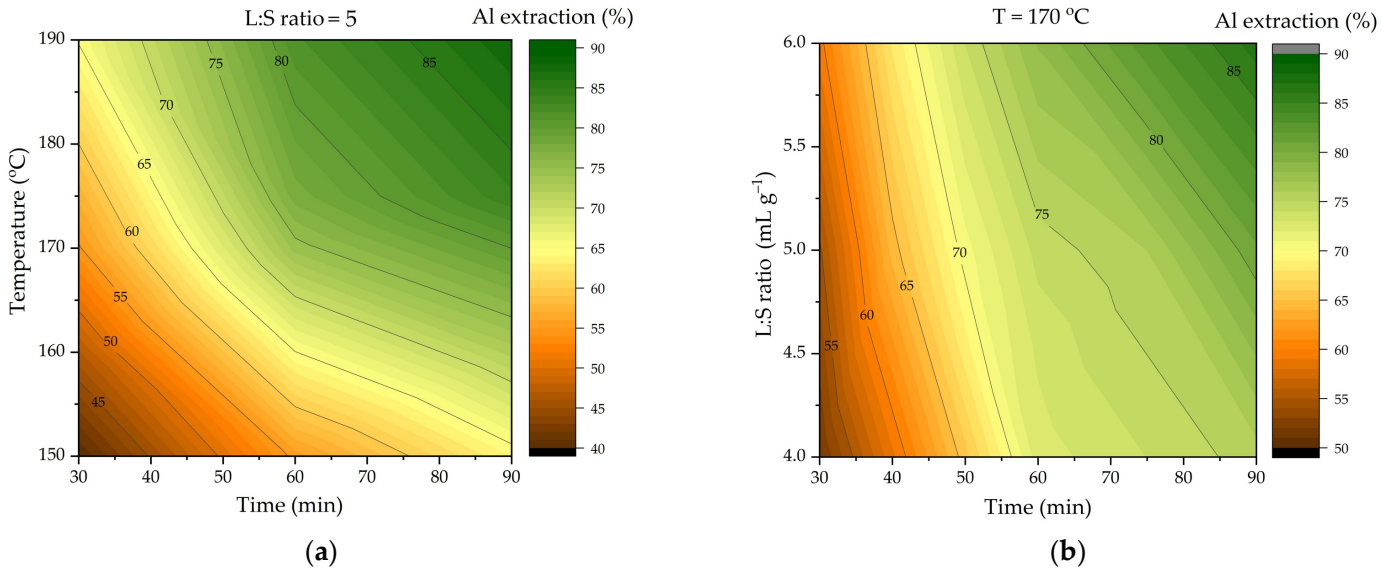


**Figure 3.** Effect of variables on Al extraction in HCl high-pressure leaching (HPAL): (**a**) effect of time and temperature at L:S ratio of 5 to 1; (**b**) effect of time and L:S ratio at 170 °C.

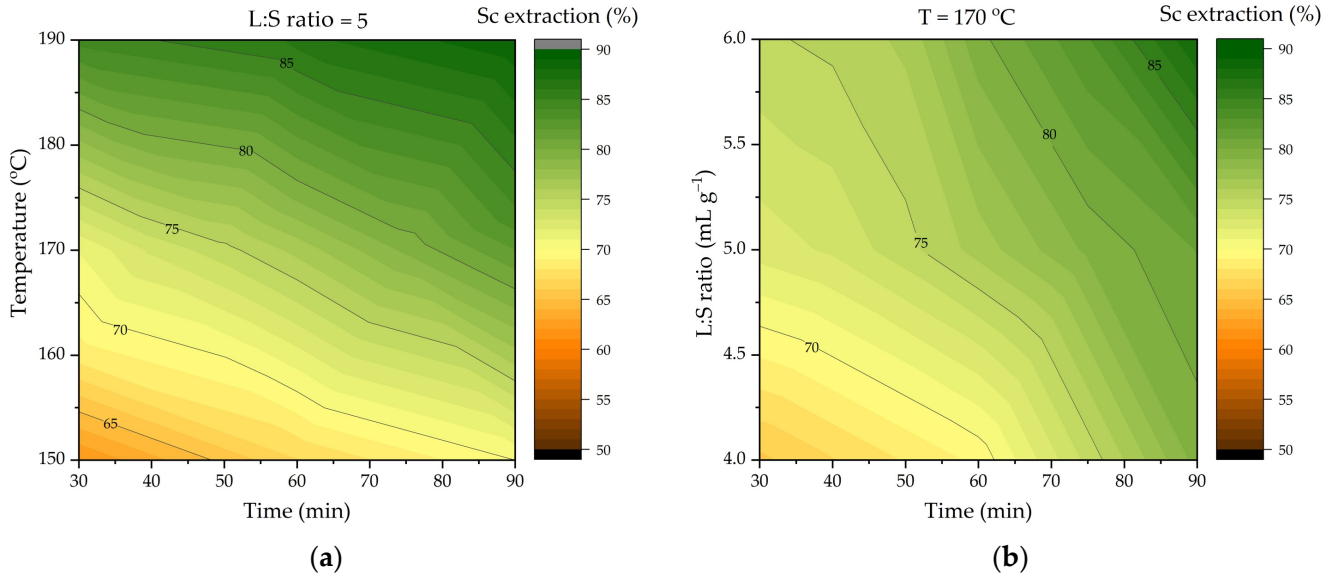


**Figure 4.** Effect of different leaching parameters on Sc extraction in HCl HPAL: (**a**) effect of time and temperature at an L:S ratio of 5 to 1; (**b**) effect of time and L:S ratio at 170 °C.

### *3.2. Leaching Kinetics*

The research was continued by studying the kinetics of the Al and Sc extraction from the DCFA. Various equations of the shrinking core model [32,33] were used to describe the process. This model is utilized to identify the limiting stage of a heterogeneous chemical reaction, which prevents the shrinkage of the initial component's core and yields a porous reaction product that can impede the diffusion of the leaching agent into the particles. The

shape of the kinetic curve allows the model to identify the limiting stage. The equations used to describe the process are as follows:

$$X = kt \text{ (external diffusion)}, \quad (2)$$

$$[1 - (1 - X)^{1/3}] = kt \text{ (surface chemical reaction)}, \quad (3)$$

$$[1 - 2/3X - (1 - X)^{2/3}] = kt \text{ (internal diffusion)}. \quad (4)$$

where X is the share of leaching; k is the rate constant, 1/s; t—time, s. Figure 5 shows the fitting of the experimental data obtained using Equations (2)–(4).

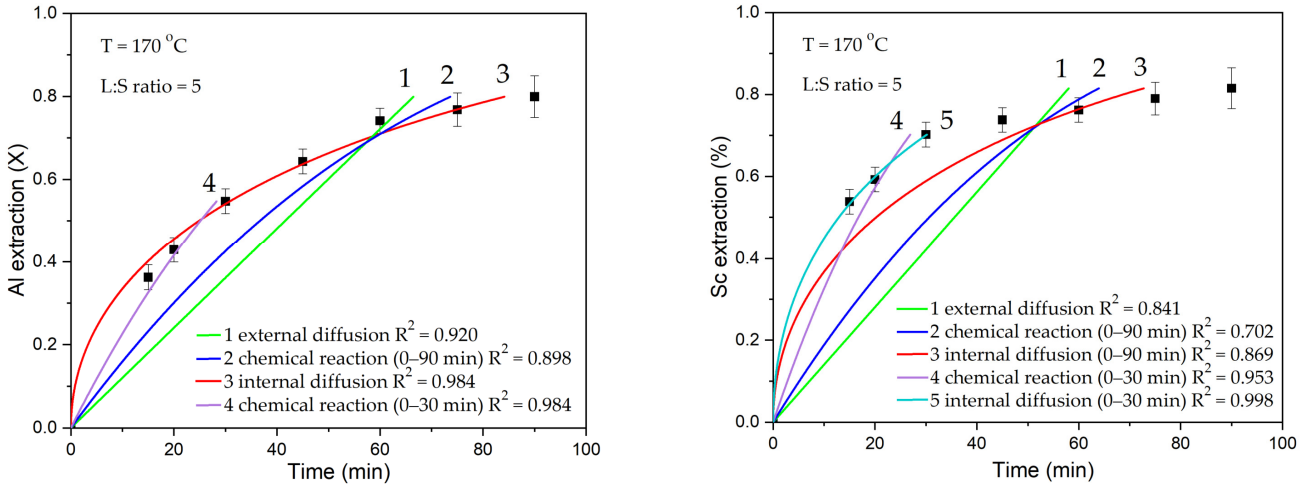


**Figure 5.** The results of fitting data (points) to different equations of shrinking core model (SCM) (lines): (**a**) extraction of Al; (**b**) extraction of Sc.

The results of the fitting in Figure 5 show that the internal diffusion model is the most suitable for describing the process at the average temperature. Nonetheless, when describing the initial 30 min of leaching, Equation (3) for the surface chemical reaction is more appropriate. When the product layer is not large enough at the beginning of the process, the reaction itself can limit the dissolution of Al from the mullite. When the core is compressed, the reagent inside the particle or the product outside slows down the leaching process.

Figure 5b shows that, for Sc extraction, the dissolution proceeds very rapidly during the initial leaching time, and, eventually, saturation is reached. Fitting becomes difficult, but the internal diffusion equation still fits better. When describing the initial 30 min of leaching, the internal diffusion equation also exhibits a highly satisfactory fit.

The results of fitting the data to the internal diffusion equation at different temperatures and L:S ratios are shown in Figure 6a,c. It is evident that the model is suitable to describe the process at all temperatures and L:S ratios. The Arrhenius equation (Equation (5)) was used to determine the apparent activation energy of the leaching based on the obtained values of the chemical reaction rate constant.

$$k = k_0 \exp(-E_a/RT). \quad (5)$$

where k—rate constant, $s^{-1}$; $E_a$—apparent activation energy, kJ $mol^{-1}$; R—universal gas constant, J $K^{-1} \cdot mol^{-1}$; T—temperature, K.

It can be seen that at low temperatures (150–170 °C), the activation energy is 52.78 kJ $mol^{-1}$. At high temperatures (170–190 °C), the mechanism changes, and the

activation energy decreases to 26.34 kJ mol$^{-1}$. This is attributable to the rapid leaching at elevated temperatures, which in turn leads to the rapid expansion of the product's inert layer.

By plotting the graph in the coordinates lnk—lnγ (logarithm of the rate constant versus logarithm of the L:S ratio), the order of the L:S ratio was determined to be 0.882. The modest effect of the L:S ratio on the rate of the process suggests a small effect of external diffusion on the process for a given concentration of HCl.

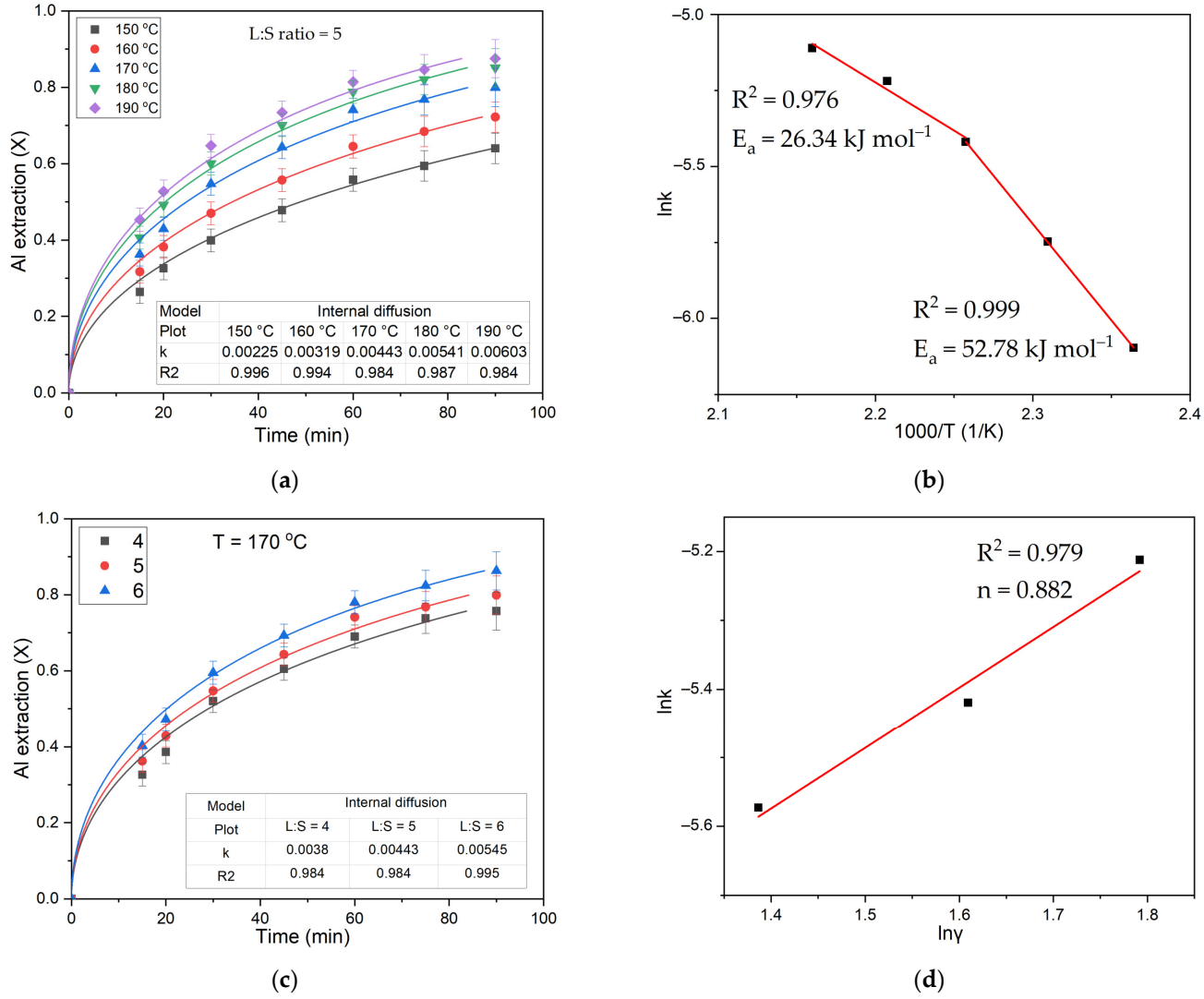


**Figure 6.** The results of fitting experimental data (points) of Al extraction to equation for the internal diffusion (lines): (**a**) the diffusion through the product layer for the effect of temperature; (**b**) relation between logarithm of rate constant and the reverse temperature; (**c**) the diffusion through the product layer for the effect of L:S ratio; and (**d**) relation between logarithm of rate constant and logarithm of L:S ratio.

As demonstrated in previous studies [31,34], the initial desilication of CFA particles facilitates the conversion of REEs into a readily soluble form after the removal of the amorphous glassy mass from the surface of CFA particles. Therefore, Sc extraction using the HPAL process is intensive, especially at T = 190 °C (Figure 7). As a result, the equations of the shrinking core model are poorly suited to describe the leaching process. Therefore, the data obtained were not used to estimate the activation energy and the L:S ratio order.

### *3.3. Solid Residue Characterisation*

To discover the solid phase, which may be an inert product that limits diffusion, the residue from the HCl leaching of DCFA was examined. The XRD patterns of DCFA residues after the HPAL process at different temperatures and leaching times are shown in Figure 8. It is evident that the XRD pattern of residue obtained at a temperature of 150 °C after a duration of 5 min of leaching exhibits no significant changes in comparison to the raw DCFA sample. A significant decrease in the intensity of the mullite peaks is observed after 15 min of leaching at T = 170 °C. This is likely to explain the high Al extraction rates at the initial moment of leaching.

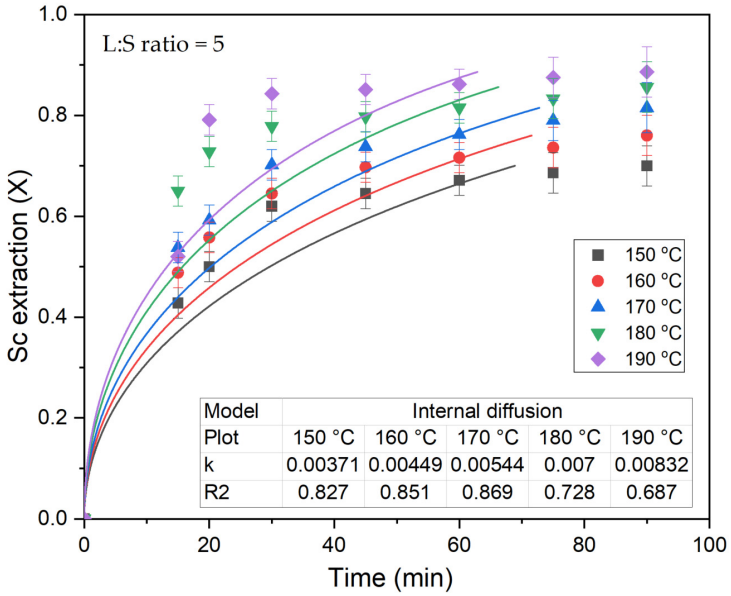


**Figure 7.** The results of fitting experimental data (points) of Sc extraction to equation for the internal diffusion (lines).

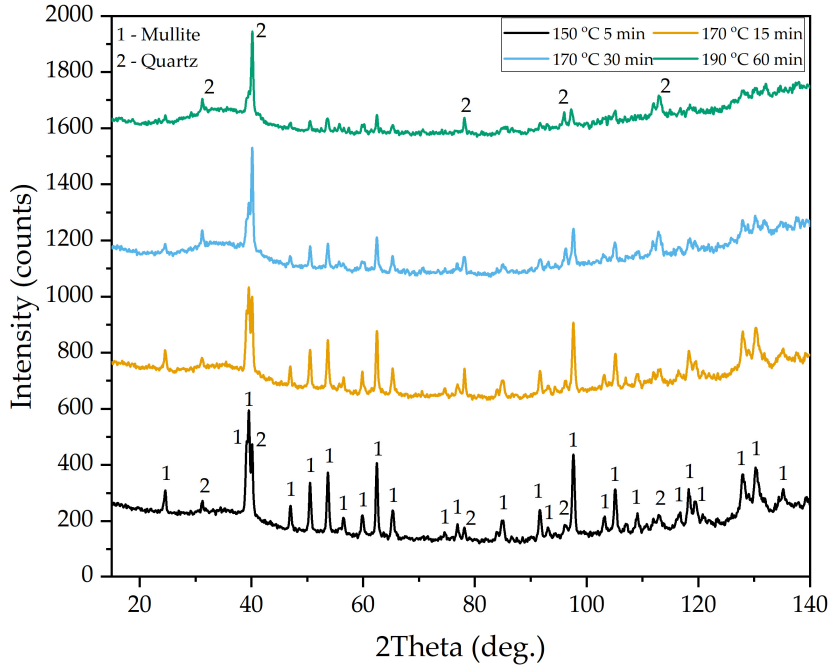


**Figure 8.** XRD patterns of DCFA leaching residue after HPAL process at different temperatures and times.

The exposure of mullite particles after the desilication process and its high surface area of 40.2 $m^2$ $g^{-1}$ (Table 3) enhanced the leaching kinetics. After 30 min of leaching at the same temperature, a small amount of mullite was left. To completely dissolve the mullite phase, more than 60 min of leaching at 190 °C was required. This fact confirms that the rate-limiting step in the late stages of Al leaching is diffusion.

The data presented in Table 3 demonstrate that the number and size of pores in the DCFA residue following HCl leaching significantly enhances its specific surface area. The increase in leaching time from 5 to 60 min and temperature from 150 °C to 190 °C does not increase the specific surface area. On the contrary, it exhibits a slight decrease. The residue remaining after HCl leaching is unlikely to be quartz, as it is represented by separate particles in the raw CFA [29]. At the same time, an amorphous phase (in the range of 30°–40°) appears on the XRD pattern of the residue obtained at T = 170 °C and 190 °C. This can be the amorphous silica phase that remains after the Al is extracted from mullite. Therefore, amorphous silica may be the product that prevents acid diffusion into the core of the unleached mullite.

**Table 3.** The physical properties of DCFA and the residue after HPAL process.

| Sample | Specific Surface Area ($m^2$ $g^{-1}$) | Pore Volume ($cm^3$ $g^{-1}$) | Pore Diameter (nm) |
|---|---|---|---|
| DCFA | 14.9 | 37.0 | 17.7 |
| Residue at T = 150 °C, τ = 5 min | 44.1 | 130.0 | 69.3 |
| Residue at T = 170 °C, τ = 15 min | 40.2 | 129.0 | 69.0 |
| Residue at T = 170 °C, τ = 30 min | 41.5 | 132.0 | 69.2 |
| Residue at T = 190 °C, τ = 60 min | 40.4 | 128.0 | 69.2 |

Table 4 shows the chemical composition of the solid residue obtained after 30 min of leaching at 170 °C. It can be seen that the solid residue is mainly composed of silicon and can be used to produce silica white [35–37] or silicon carbide ceramics [38–40].

**Table 4.** Chemical composition of the solid residue after 30 min of leaching at 170 °C.

| Sample | Components (wt.%) | | | | | | | | | | |
|---|---|---|---|---|---|---|---|---|---|---|---|
| | $SiO_2$ | $Al_2O_3$ | CaO | $Fe_2O_3$ | $TiO_2$ | MgO | $Na_2O$ | $K_2O$ | LOI | Sc | C |
| HPAL solid residue | 71.96 | 13.94 | 2.27 | 2.19 | 3.26 | 0.28 | 0.36 | 0.03 | 5.30 | 0.0009 | 4.70 |

Figure 9 shows the SEM-EDS images of the product resulting from the HCl leaching at temperatures of 170 °C and 190 °C. The residue obtained at 170 °C contains, on average, more Al than the sample obtained at T = 190 °C (Figure 9a). Figure 9b shows that on the mullite surface, there are areas with a minimum Al and maximum Si content. The residue obtained at 190 °C is highly corroded (Figure 9c). The surface of mullite particles exhibits a greater degree of smoothness in comparison to particles obtained at a temperature of T = 170 °C. This fact could explain a certain decrease in the specific surface area of the residue sample (Table 3). The limitation of the process is caused by internal diffusion, which suggests that mechanical activation could be employed to further enhance the process [25].

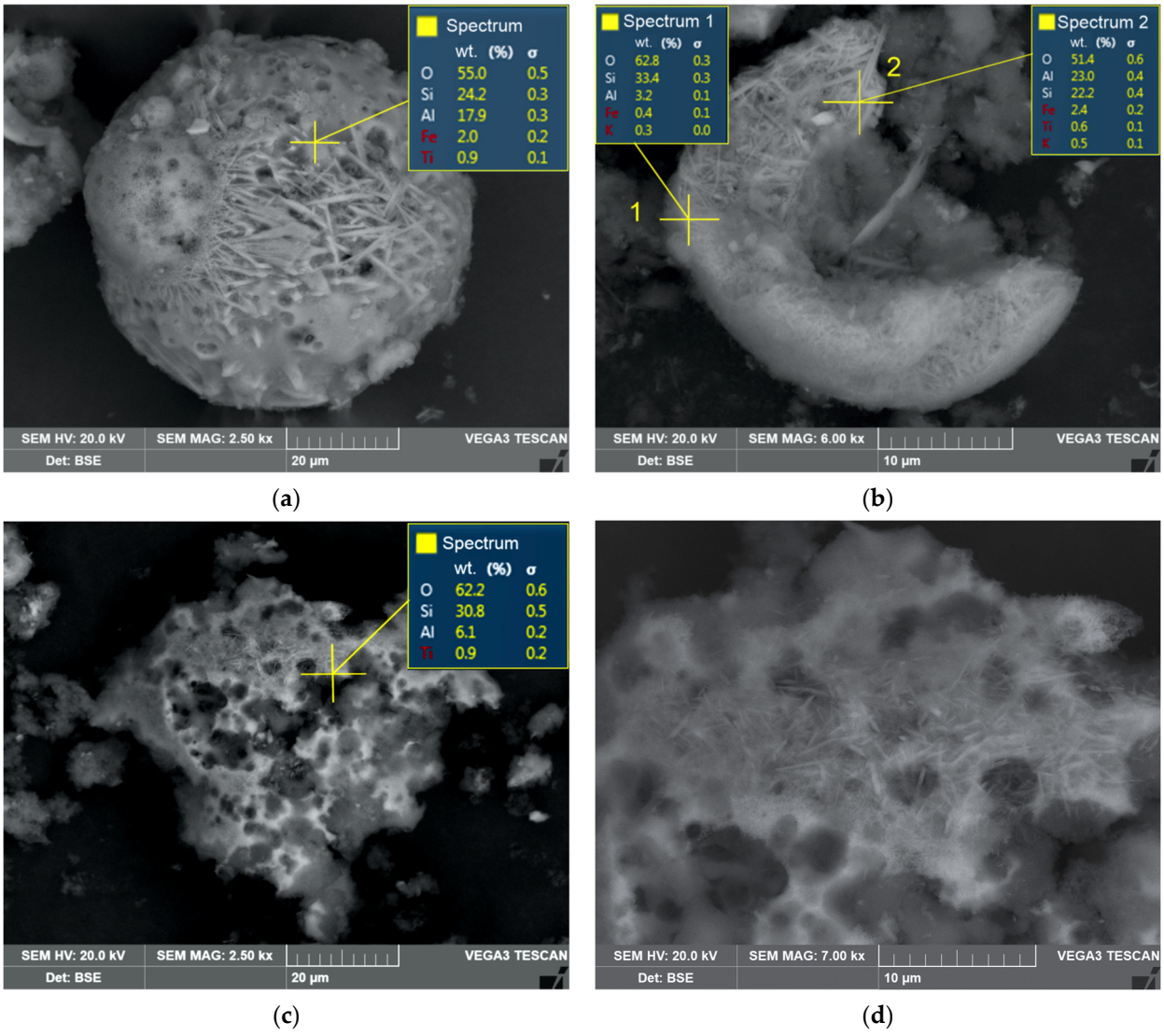


**Figure 9.** SEM-EDS images of (**a**) solid residue after 15 min of leaching at 170 °C, a magnitude of 2500×; (**b**) solid residue after 15 min of leaching at 170 °C, a magnitude of 6000×; (**c**) solid residue after 60 min of leaching at 190 °C, a magnitude of 2500×; (**d**) solid residue after 60 min of leaching at 190 °C, a magnitude of 7000×.

## 4. Conclusions

The kinetics of the HPAL process for preliminary desilicated CFA were investigated in this study. The main conclusions are as follows:

1. After 90 min of leaching, more than 80% of Al and Sc can be extracted from desilicated coal fly ash at 170 °C. The kinetic results obtained at various temperatures showed that Al dissolution follows the surface chemical reaction and diffusion-controlled shrinking core models during the initial and later stages of leaching, respectively. At low temperatures, a high activation energy of 52.78 kJ $mol^{-1}$ was observed, then a change in the mechanism occurred when the activation energy decreased to 26.34 kJ $mol^{-1}$.
2. The extraction of Sc from desilicated CFA in the high-pressure leaching process is very intense, especially at high temperatures. As a result, the equations of the shrinking core model are poorly suited to describe the process. Amorphous silica may be the product that prevents acid diffusion inside the particles to the core of unleached mullite, according to the results of SEM-EDS analysis.

**Author Contributions:** Conceptualization, A.S. and I.L.; methodology, A.S.; software, D.V.; validation, D.V.; formal analysis, I.L.; investigation, A.S.; resources, A.S.; data curation, A.S.; writing—original draft preparation, A.S. and D.V.; writing—review and editing, D.V.; visualization, A.S.; supervision, I.L.; project administration, A.S.; funding acquisition, A.S. All authors have read and agreed to the published version of the manuscript.

**Funding:** This research was supported by the Russian Science Foundation and Government of Sverdlovsk region, Joint Grant No 22-23-20150.

**Data Availability Statement:** Data are contained within this article.

**Acknowledgments:** The authors thank Evgeny Kolesnikov from NUST MISiS for his help with the SEM and XRD studies of the solid samples.

**Conflicts of Interest:** The authors declare no conflict of interest.

## References

1. Das, D.; Rout, P.K. A Review of Coal Fly Ash Utilization to Save the Environment. *Water Air Soil Pollut.* **2023**, *234*, 128. [CrossRef]
2. Kamara, S.; Foday Jr, E.H.; Wang, W. A Review on the Utilization and Environmental Concerns of Coal Fly Ash. *Am. J. Chem. Pharm.* **2023**, *2*, 53–65. [CrossRef]
3. Bhatt, A.; Priyadarshini, S.; Acharath Mohanakrishnan, A.; Abri, A.; Sattler, M.; Techapaphawit, S. Physical, Chemical, and Geotechnical Properties of Coal Fly Ash: A Global Review. *Case Stud. Constr. Mater.* **2019**, *11*, e00263. [CrossRef]
4. Zierold, K.M.; Odoh, C. A Review on Fly Ash from Coal-Fired Power Plants: Chemical Composition, Regulations, and Health Evidence. *Rev. Environ. Health* **2020**, *35*, 401–418. [CrossRef] [PubMed]
5. Li, S.; Bo, P.; Kang, L.; Guo, H.; Gao, W.; Qin, S. Activation Pretreatment and Leaching Process of High-Alumina Coal Fly Ash to Extract Lithium and Aluminum. *Metals* **2020**, *10*, 893. [CrossRef]
6. Navagire, O.P.; Sharma, S.K.; Rambabu, D. Stabilization of Expansive Soil with Thermal Power Plant Waste (Fly Ash and Coal Bottom Ash)—A Review. In *Advances in Chemical, Bio and Environmental Engineering*; Ratan, J.K., Sahu, D., Pandhare, N.N., Bhavanam, A., Eds.; Environmental Science and Engineering; Springer International Publishing: Cham, Switzerland, 2022; pp. 323–332, ISBN 978-3-030-96553-2.
7. Yusop, H.; Suhatril, M.; Abdul Hamid, M.A.H.; Zainal, F.; Fauzan, M.d.; Yapandi, M.F.K.; Abbas, N.A. Usage of Coal Fly Ash and Bottom Ash from Ash Ponds for Bricks and Precast Concrete Blocks—A Review. *J. Ssustain. Civil Eng. Technol.* **2022**, *1*, 50–62. [CrossRef]
8. Huang, Q.; Li, X.; Qi, T.; Peng, Z.; Liu, G.; Zhou, Q. Dynamic Expansion Experiment of Efficient Separation of Aluminum and Silicon from Coal Fly Ash. *Zhongguo Youse Jinshu Xuebao Chin. J. Nonferrous Met.* **2022**, *32*, 173–182. [CrossRef]
9. Wang, H.; Wang, J.; Li, J.; Li, Z.; Li, W.; Yang, M.; Shen, L. Mechanical Activation of Coal Fly Ash for the Improvement of Alumina–Silica Separation During Reduction Roasting–Alkaline Leaching Process. *JOM* **2023**. [CrossRef]
10. Li, X.; Wang, P.; Wang, H.; Zhou, Q.; Qi, T.; Liu, G.; Peng, Z.; Wang, Y.; Shen, L. The Alkaline Leaching Behavior of Silica Solid Solutions in the Product Obtained by Roasting the Mixture of High-Alumina Coal Gangue and Hematite. *J. Sustain. Metall.* **2022**, *8*, 1853–1865. [CrossRef]
11. Panda, L.; Dash, S.; Kar, B.; Panigrahi, S.; Mohanty, I. Alkaline Hydrothermal Synthesis of Zeolite from Class F Coal Fly Ash. *J. Solid Waste Technol. Manag.* **2021**, *47*, 674–681. [CrossRef]
12. Hanum, F.H.; Rahayu, A.; Hapsauqi, I. The Comparison Effect of NaOH and KOH as The Leaching Solution for Silica from Two Different Coal Fly Ashes. *Indo. J. Chem. Res.* **2022**, *10*, 27–31. [CrossRef]
13. Cao, Y.; Luo, J.; Sun, S. Characteristics of MSWI Fly Ash with Acid Leaching Treatment. *J. Fuel Chem. Technol.* **2021**, *49*, 1208–1218. [CrossRef]
14. Apua, M.C.; Nkazi, B.D. Leaching of Coal Fly Ash with Sulphuric Acid for Synthesis of Wastewater Treatment Composite Coagulant. *Can. Metall. Q.* **2022**, *61*, 309–331. [CrossRef]
15. Wang, P.; Liu, H.; Zheng, F.; Liu, Y.; Kuang, G.; Deng, R.; Li, H. Extraction of Aluminum from Coal Fly Ash Using Pressurized Sulfuric Acid Leaching with Emphasis on Optimization and Mechanism. *JOM* **2021**, *73*, 2643–2651. [CrossRef]
16. Liu, C.-J.; Zhao, A.-C.; Ye, X.; Zhao, Z.; Yang, X.-R.; Qin, Y.-M.; Zhang, T.-A. Kinetics of Aluminum Extraction from Roasting Activated Fly Ash by Sulfuric Acid Leaching. *MRS Commun.* **2023**. [CrossRef]
17. Kumar, A.; Agrawal, S.; Dhawan, N. Processing of Coal Fly Ash for the Extraction of Alumina Values. *J. Sustain. Metall.* **2020**, *6*, 294–306. [CrossRef]
18. Guo, Y.; Li, J.; Yan, K.; Cao, L.; Cheng, F. A Prospective Process for Alumina Extraction via the Co-Treatment of Coal Fly Ash and Bauxite Red Mud: Investigation of the Process. *Hydrometallurgy* **2019**, *186*, 98–104. [CrossRef]
19. Shi, Y.; Jiang, K.; Zhang, T. Cleaner Extraction of Alumina from Coal Fly Ash: Baking-Electrolysis Method. *Fuel* **2020**, *273*, 117697. [CrossRef]
20. Shemi, A.; Mpana, R.N.; Ndlovu, S.; Van Dyk, L.D.; Sibanda, V.; Seepe, L. Alternative Techniques for Extracting Alumina from Coal Fly Ash. *Miner. Eng.* **2012**, *34*, 30–37. [CrossRef]

21. Rui, H.; Zhang, L.; Li, L.; Zhu, L. Solvent Extraction of Lithium from Hydrochloric Acid Leaching Solution of High-Alumina Coal Fly Ash. *Chem. Phys. Lett.* **2021**, *771*, 138510. [CrossRef]
22. Smith, P. The Processing of High Silica Bauxites—Review of Existing and Potential Processes. *Hydrometallurgy* **2009**, *98*, 162–176. [CrossRef]
23. Aphane, M.E.; Doucet, F.J.; Kruger, R.A.; Petrik, L.; Van Der Merwe, E.M. Preparation of Sodium Silicate Solutions and Silica Nanoparticles from South African Coal Fly Ash. *Waste Biomass Valor.* **2019**, *11*, 4403–4417. [CrossRef]
24. Valeev, D.; Bobylev, P.; Osokin, N.; Zolotova, I.; Rodionov, I.; Salazar-Concha, C.; Verichev, K. A Review of the Alumina Production from Coal Fly Ash, with a Focus in Russia. *J. Clean. Prod.* **2022**, *363*, 132360. [CrossRef]
25. Barry, T.S.; Uysal, T.; Birinci, M.; Erdemoğlu, M. Thermal and Mechanical Activation in Acid Leaching Processes of Non-Bauxite Ores Available for Alumina Production—A Review. *Min. Metall. Explor.* **2019**, *36*, 557–569. [CrossRef]
26. Ji, H.; Mi, X.; Tian, Q.; Liu, C.; Yao, J.; Ma, S.; Zeng, G. Recycling of Mullite from High-Alumina Coal Fly Ash by a Mechanochemical Activation Method: Effect of Particle Size and Mechanism Research. *Sci. Total Environ.* **2021**, *784*, 147100. [CrossRef] [PubMed]
27. Aydoğmuş, R.; Erdemoğlu, M.; Uysal, T. Aluminum Recovery by Acid Leaching of Variously Enriched Pyrophyllite Ore: Effects of Pre-Treatment Methods for Activation. *Min. Metall. Explor.* **2023**, *40*, 1333–1343. [CrossRef]
28. Rezaei, H.; Ziaedin Shafaei, S.; Abdollahi, H.; Shahidi, A.; Ghassa, S. A Sustainable Method for Germanium, Vanadium and Lithium Extraction from Coal Fly Ash: Sodium Salts Roasting and Organic Acids Leaching. *Fuel* **2022**, *312*, 122844. [CrossRef]
29. Shoppert, A.; Loginova, I.; Valeev, D. Kinetics Study of Al Extraction from Desilicated Coal Fly Ash by NaOH at Atmospheric Pressure. *Materials* **2021**, *14*, 7700. [CrossRef]
30. Shoppert, A.; Valeev, D.; Loginova, I.; Chaikin, L.; Pan, J. Enhanced Coal Fly Ash Desilication Using Atmospheric NaOH Leaching with Simultaneous Magnetic Separation. *Metals* **2023**, *13*, 1647. [CrossRef]
31. Shoppert, A.; Valeev, D.; Napol'skikh, J.; Loginova, I.; Pan, J.; Chen, H.; Zhang, L. Rare-Earth Elements Extraction from Low-Alkali Desilicated Coal Fly Ash by $(NH_4)_2SO_4$ + $H_2SO_4$. *Materials* **2022**, *16*, 6. [CrossRef]
32. Levenspiel, O. *Chemical Reaction Engineering*, 3rd ed.; Wiley: New York, NY, USA, 1999; ISBN 978-0-471-25424-9.
33. Gok, O.; Anderson, C.G.; Cicekli, G.; Cocen, E.I. Leaching Kinetics of Copper from Chalcopyrite Concentrate in Nitrous-Sulfuric Acid. *Physicochem. Probl. Miner. Process.* **2014**, *50*, 399–413. [CrossRef]
34. Trinh, H.B.; Kim, S.; Lee, J. Recovery of Rare Earth Elements from Coal Fly Ash Using Enrichment by Sodium Hydroxide Leaching and Dissolution by Hydrochloric Acid. *Geosystem Eng.* **2022**, *25*, 53–62. [CrossRef]
35. Yadav, V.K.; Amari, A.; Mahdhi, N.; Elkhaleefa, A.M.; Fulekar, M.H.; Patel, A. A Novel and Economical Approach for the Synthesis of Short Rod-Shaped Mesoporous Silica Nanoparticles from Coal Fly Ash Waste by Bacillus Circulans MTCC 6811. *World J. Microbiol. Biotechnol.* **2023**, *39*, 289. [CrossRef] [PubMed]
36. Yadav, V.K.; Amari, A.; Wanale, S.G.; Osman, H.; Fulekar, M.H. Synthesis of Floral-Shaped Nanosilica from Coal Fly Ash and Its Application for the Remediation of Heavy Metals from Fly Ash Aqueous Solutions. *Sustainability* **2023**, *15*, 2612. [CrossRef]
37. Imoisili, P.E.; Jen, T.-C. Microwave-Assisted Sol–Gel Template-Free Synthesis and Characterization of Silica Nanoparticles Obtained from South African Coal Fly Ash. *Nanotechnol. Rev.* **2022**, *11*, 3042–3052. [CrossRef]
38. Xiao, J.; Li, F.; Zhong, Q.; Bao, H.; Wang, B.; Huang, J.; Zhang, Y. Separation of Aluminum and Silica from Coal Gangue by Elevated Temperature Acid Leaching for the Preparation of Alumina and SiC. *Hydrometallurgy* **2015**, *155*, 118–124. [CrossRef]
39. Hongjie, W.; Yonglan, W.; Zhihao, J. SiC Powders Prepared from Fly Ash. *J. Mater. Process. Technol.* **2001**, *117*, 52–55. [CrossRef]
40. Sulardjaka; Jamasri; Wildan, M.W.; Kusnanto. Method for Increasing β-SiC Yield on Solid State Reaction of Coal Fly Ash and Activated Carbon Powder. *Bull. Mater. Sci.* **2011**, *34*, 1013–1016. [CrossRef]